An Effective SAR Reduction Technique of a Compact Meander Line Antenna for Wearable Applications

Shankar Bhattacharjee*, Monojit Mitra, and Sekhar R. Bhadra Chaudhuri

Abstract—In this paper, a symmetrically structured meander line antenna placed around a T-shaped junction with truncated ground planes is proposed for wearable applications. The designed antenna has a percentage bandwidth of 69.04% covering the GSM 1800 band industrial scientific and medical (ISM) 2.4–2.5 GHz band, 4G LTE band 7 (2.5–2.69 GHz). The antenna is compact in nature with a size of $30 \times 40 \times 1.6 \, \text{mm}^3$. SAR reduction is achieved without the attachment of any additional unit. It is found that the application of designed truncated ground planes around positions of high electric field (E-field) region is an effective solution for reduction of Specific Absorption Rate (SAR) significantly through field cancellation technique. Maximum temperature elevation due to electromagnetic wave absorption has also been computed. The antenna is simulated over a homogenous human dry skin model as well as over a head model. The proposed design is fabricated and measured, and it is found to be compatible for real world applications while considering its miniaturization, radiation patterns and SAR limitations.

1. INTRODUCTION

The medical industry has revealed massive innovations and modernizations in recent years. With the advancements of technologies, real time monitoring of patients is now possible from distant places through wireless communication. An antenna is a major module in any wearable system which determines the overall performance of the system. Therefore, the design of a proper antenna for effective communication link is of prime importance. The principal constraints in designing wearable antennas are frequency detuning, impedance mismatch, radiation effect over human body, bandwidth degradation, moisture absorption and bending effects. Human tissue is lossy in nature. Due to its high permittivity value, the resonant frequency of the antenna shifts, and the radiation pattern gets distorted further. The requirement of high transmission rate at short ranges signifies the need of wideband feature with respect to wearable antenna. Several bandwidth enhancement techniques have been implemented using rigid substrates such as parasitic coupling and inductive loading [1], asymmetrical slots with CPW feed and microstrip feed [2] and with non-rigid substrates in [3, 4]. The wideband antenna in [3] incorporates a T-shaped monopole antenna with parasitic elements for bandwidth enhancement.

Since wearable antennas work in close vicinity of human body, the associated health hazards with electromagnetic (em) waves have also been reported earlier. For reduction of em wave exposure, various SAR reduction techniques have been used in the past viz. the use of ferrite sheets to reduce the surface currents [5], metamaterial ground to act as stopband in the operating frequency range [6] and integrating electromagnetic band gap structures to behave as reflectors in reducing the SAR [7]. In [8], the use of metal rods to generate anti-phase fields with the antenna was found effective in SAR reduction where the lateral size of the system was increased. R-cards were used in [9] where SAR reduction was achieved with degradation of radiation efficiency. Recently, magneto-dielectric nano composite materials as substrate were used in [10] to reduce the SAR. Although the use of the above techniques is successful in reduction

of SAR, the design is complex, and the size of the antenna also increases. Further, the additional units used for SAR reduction either act as reflectors or absorbers which may also hamper communication performance in the reverse direction.

The proposed work mainly addresses the issue of SAR in addition to bandwidth enhancement for wearable antennas. A symmetrical dual meander line antenna having a T-shaped junction and truncated ground plane is proposed. CPW feeding technique with reduced ground plane is used in order to obtain a horizontal monopole like bidirectional radiation beam when being placed over human body. Most of the previous designs used PEC ground plane, metamaterial ground and AMC ground for reducing the exposure of radiation over human body. However, in our design, initially a single resonant mode is generated with a simple T-shaped structure at the end of the antenna. A pair of symmetrical stubs is added near the feed line so that higher order mode is generated. Thereafter, meandering the stub results into miniaturization in higher mode of the antenna. The miniaturization of the higher-order mode and merging with the lower mode results into realization of a wideband antenna. Finally, a SAR reduction technique with variation in the geometry of the ground plane in order to reduce the effects of high E-field regions through field cancellation technique is presented. The SAR reduction technique is achieved by keeping bidirectional radiation pattern and other antenna parameters in order. The validation of SAR reduction is confirmed by simulating the antennas in two solvers that are COMSOL Multiphysics using the head model and ANSYS High Frequency Structural Simulator (HFSS) with the hand model.

2. ANTENNA STRUCTURE AND DESIGN

For proof of the concept, the antenna is designed over an FR-4 substrate with dielectric constant 4.4 and height 1.6 mm. Fig. 1 shows the evolution of design of the antenna.
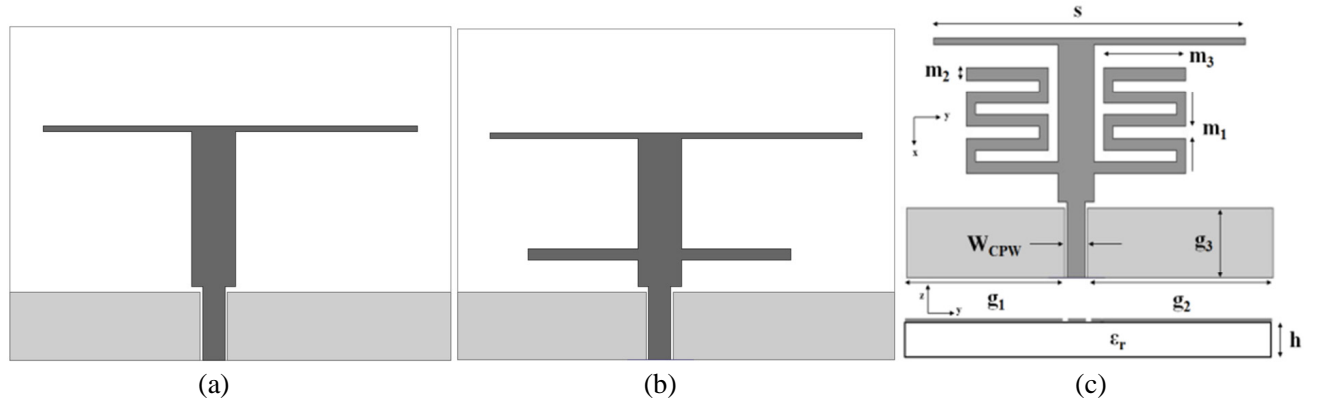

Figure 1. (a), (b), (c) Evolution of the initial design.

The antenna is fed with a $50\,\Omega$ CPW transmission line. The overall dimension of the antenna is $30 \times 40 \times 1.6\,\text{mm}^3$. The design equation of the CPW feeding line is derived from [11]. It is desired initially to generate a dual-band antenna with considerable band separation between them and then merging out those two bands resulting into a wideband antenna response. Principally, the lower order band is left unaffected, and the higher order band is chosen to be miniaturized in order to unify both the bands. In this context, a simple prototype of T-shaped CPW-fed patch antenna having a resonant frequency of 2.1 GHz is designed initially. The surface current mainly flows over the T-junction which can be seen from the current distribution plot in Fig. 2(a). In order to generate another mode, a small section from the T-shaped patch is extended in both sides near the feed point as shown in Fig. 2(d) which is the 2nd prototype. It can be realized that higher order mode is generated due to the current flow in the shorter arm, and lower one will be that of upper or longer arm as shown in Fig. 2(e) since the resonant frequency is inversely proportional to the current path length. The higher order mode of the antenna is non-radiating initially as the impedance is not matched in this case which can be verified from Smith chart plot in Figs. 2(b)&(c).
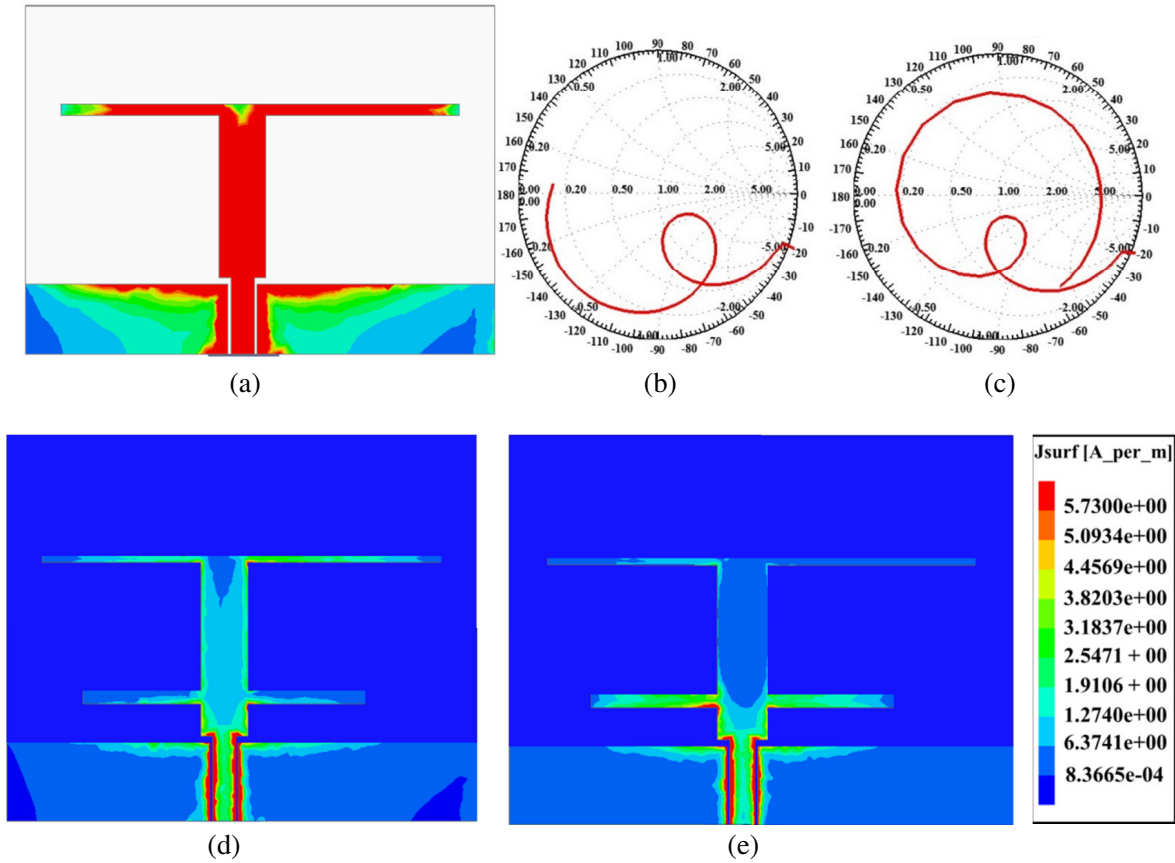
Figure 2. (a) Surface current distribution at 2.1 GHz, Smith Chart for prototype, (b) 1st, (c) 2nd, (d), (e) current distribution at 2.1 GHz and 4 GHz.

3. MINIATURIZATION AND BANDWIDTH ENHANCEMENT

In order to miniaturize the higher order mode, substantial meandering is done along the lower arm which is responsible for the higher order mode generation. Each turn of the meander follows the relation given by

$$l = 2m_3 + m_1 \tag{1}$$

where l is the length of each meander turn, $m_1 = 1\,\mathrm{mm}$, $m_3 = 9\,\mathrm{mm}$.

Detailed dimensions of the designed antenna in Fig. 1(c) are given in Table 1. A set of parametric studies is performed to find the best results with the antenna.

Table 1. Dimensions of the antenna.

Symbol	s	g_1	g_2	g_3	h	m_1	m_2	m_3	W_{cpw}
Dimensions (in mm)	34	20.28	17.28	6	1.6	1	1	9	2

It is found that the higher order resonating frequency of the antenna follows almost a linear pattern with the meander length as shown in Fig. 3(a). Thus increasing the meander length (number of turns) results into considerable miniaturization. The return loss plot versus frequency is plotted in Fig. 3(b) with varying numbers of turns for the meander antenna. The higher mode for the 1 by 1 meander case is initially non-resonating which is indicated by the rightmost vertical red arrow in Fig. 3(b). The resistive impedance of the antenna is too low in this case, so matching is not worthy for the second band. As the number of turns of the meander line is increased, the second order mode starts resonating and
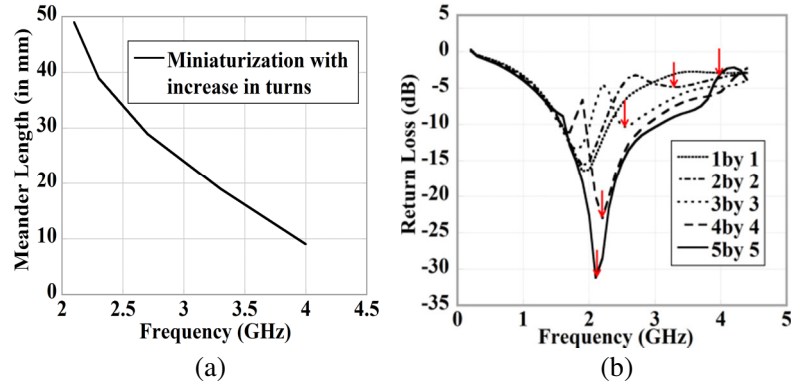
Figure 3. (a) Variation in higher order resonant frequency with meander length, (b) S_{11} variation with turns.
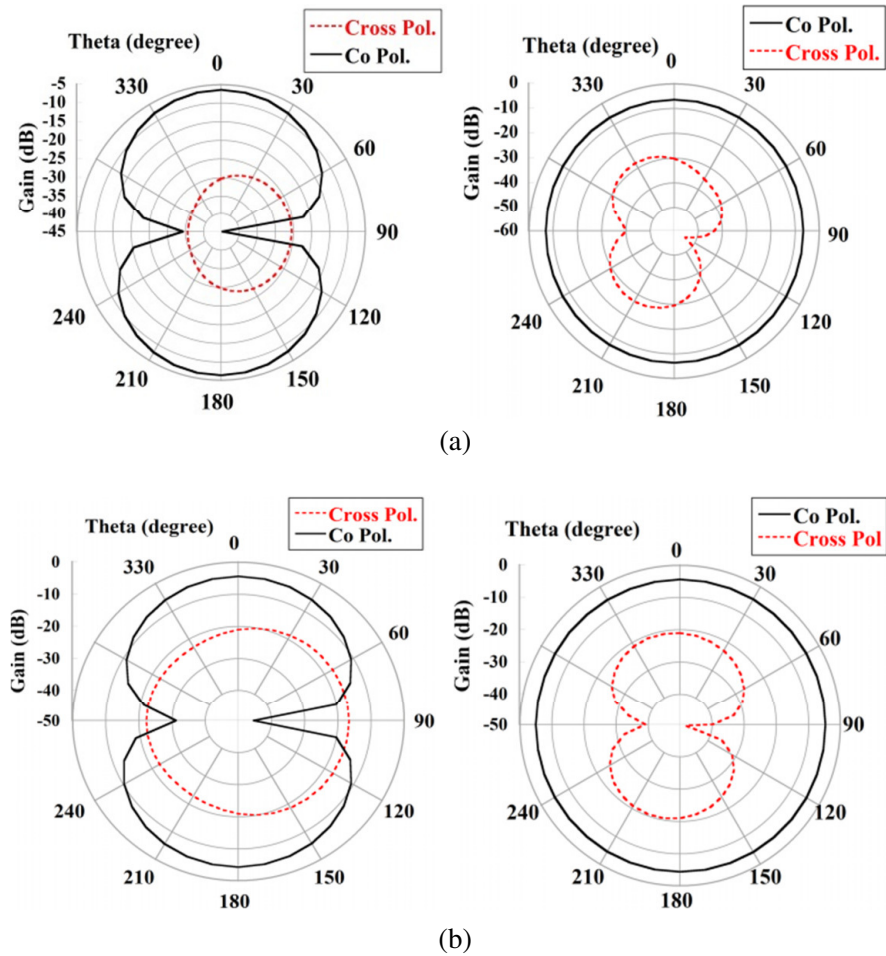

(a)

(b)

Figure 4. Radiation patterns: E-plane and H-plane, (a) 1.8 GHz, (b) 2.4 GHz.

subsequently gets miniaturized. However, the first order mode due to the upper arm is less affected. At a certain frequency, the two modes get merged resulting into wide bandwidth, and improved matching is obtained. The input resistance of the antenna gets enhanced due to increase in number of bends [12] over the meander antenna. The calculated efficiency of the final proposed antenna is 96.9%. Miniaturization of 44.7% is obtained for the higher band.

Radiation performance of the antenna is plotted for different operating frequencies in Fig. 4. To characterize the radiation pattern at application bands, two frequencies are taken, i.e., 1.8 GHz and 2.4 GHz.

The E-plane radiation pattern is bidirectional, and H-plane radiation pattern is almost omnidirectional in nature. There is excellent isolation between co pol. and cross pol. in H-plane where as in E-plane there is little merging between them in the end-fire direction, but the broadside pattern remains unaffected.

4. E-FIELD CANCELLATION & SAR REDUCTION TECHNIQUE

SAR is a standardized metric used to measure the effect of radiation over human body. The standard threshold value below which an antenna is SAR safe has been defined by IEEE in [13] which is 1.6 W/kg for 1 gm average and 2 W/kg for 10 gm average. The electric field distribution over any surface including both the near and far fields is given by [14]:

$$\vec{E} = \frac{1}{j\omega\mu\varepsilon}\left[k^2\vec{A} + \nabla(\nabla \cdot \vec{A})\right] \tag{2}$$

where $\vec{A}$ is the magnetic vector potential, k the wave number, and ω, μ, ε are the frequency, permeability and permittivity of the free space, respectively.

The near-field component is dependent on double derivative of the vector potential. This results into increase in electric field in points of edge discontinuity. So in meander line antenna at every turning point there is chances of enhanced electric field and subsequently high SAR value which is directly dependent on the electric field as given by the following equation:

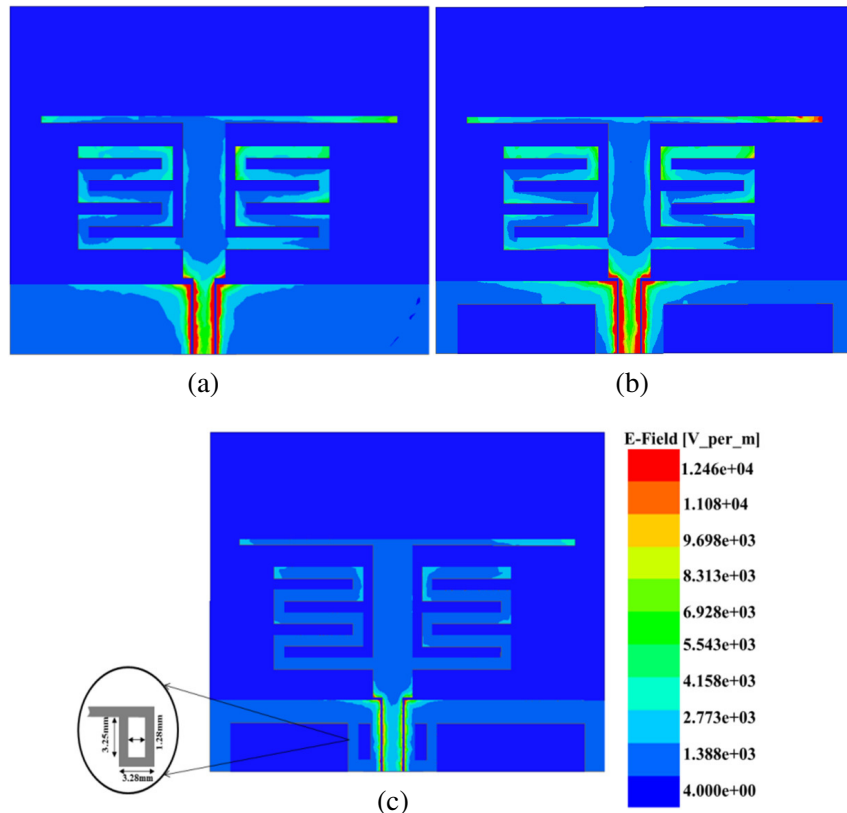$$\text{SAR} = \frac{\sigma E_{\text{rms}}^2}{\rho} \tag{3}$$

Figure 5. E-field at 2.1 GHz for (a) simple ground, (b) inverted U-shape ground, (c) truncated ground.

where σ, E_{rms}, ρ are the conductivity of the human tissue, rms value of the induced electric field and density of the human tissue.

SAR is directly dependent on square of the induced electric field which means that a higher electric field within a confined region may result into higher SAR value. It is known that input power applied over the antenna can control the SAR value. Also the extent of E-field variation can be used to track the values of SAR. The general objective in this case is to reduce or distribute the magnitude of high electric field regions which are caused by edge discontinuities without affecting the radiation performance of the antenna. Simulations were performed using ANSOFT HFSS software. It can be seen that maximum electric field of the antenna is confined around the portion comprising the feed line and ground plane in Fig. 5(a). The structure of the feed line is not changed due to the matching requirement. However, the ground plane is optimally varied in order to reduce the high electric field or distribute the same. In the next step, the ground plane is truncated parametrically, and it is found that an inverted dual U-shape ground is capable of reducing the electric field around the confined area as given in Fig. 5(b). In the 3rd case, meandering the arm near the feed line results in forming a loop around that point. It is known that adjacent arms of the meander line have opposite phases [15]. So by introduction of single meander, turn around the position of maximum electric field and joining with the inverted ground section can easily reduce the electric field magnitude at that point which can be verified from the electric field distribution plot in Fig. 5(c). The dimensions of the meander turn is optimized stepwise for obtaining proper phase accordingly. The variation of ground planes is found to have minimum effect over antenna performance.

5. FABRICATION AND MEASUREMENT RESULTS

The fabricated antenna is shown in Fig. 6(a). The measured and simulated S_{11} parameter results of the proposed antenna are plotted in Fig. 6(b).
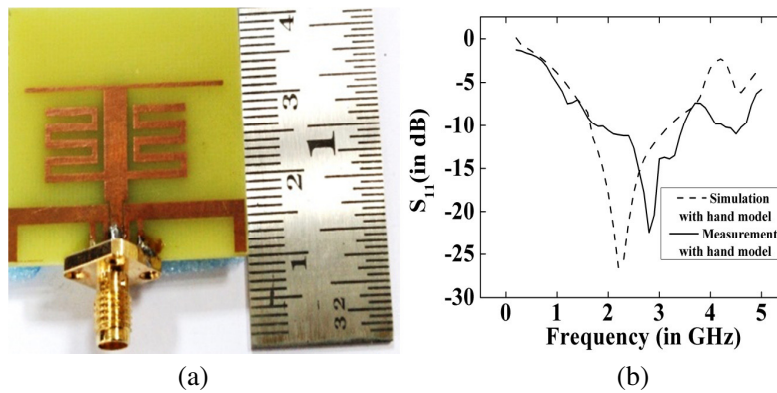

(a)   (b)

Figure 6. (a) Fabricated antenna, (b) simulated and measured S_{11} plot.

It is observed that although S_{11} of the antenna decreases, and frequency shifts when being placed over human hand, the antenna is still able to cover the required application bandwidth efficiently. The slight change in resonating frequency of the antenna is due to fabrication constraint.

6. SAR CALCULATION IN DIFFERENT MODULES

In order to validate our proposition, simulations for SAR were performed with head model placed at a distance of 2 mm from the antenna. Fig. 7 gives the simulation results of the antenna in COMSOL Multiphysics Solver with RF module and heat transfer module. The whole brain is divided into slices, and the SAR value is computed over each layer. Results show that the SAR is reduced when the truncation of ground planes is performed (shown in Fig. 7(c)) over the simple ground plane and inverted U-ground as shown in Figs. 7(a) and 7(b). Although the SAR values obtained with the two modules are different, the results show reduction in SAR values for both the cases.
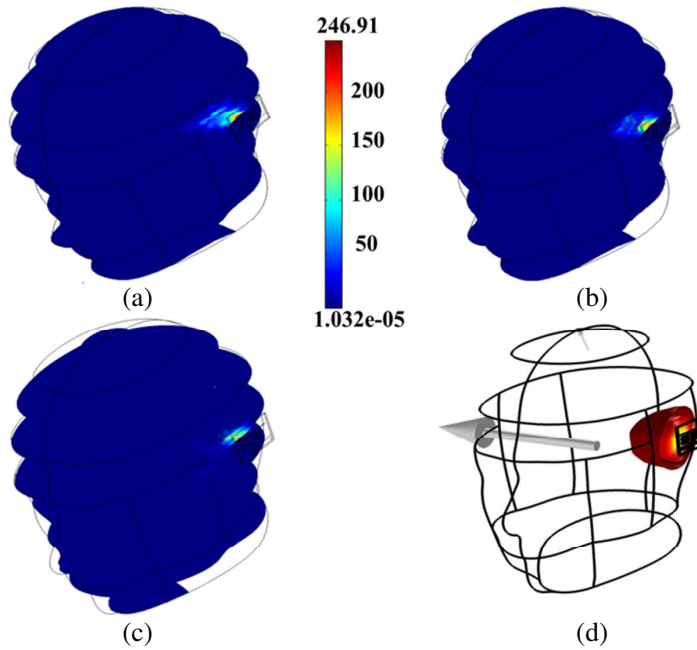
Figure 7. SAR plots in COMSOL multiphysics for (a) plane ground, (b) inverted U-shape ground, (c) truncated ground plane, (d) direction of heat flux plot of the final antenna.
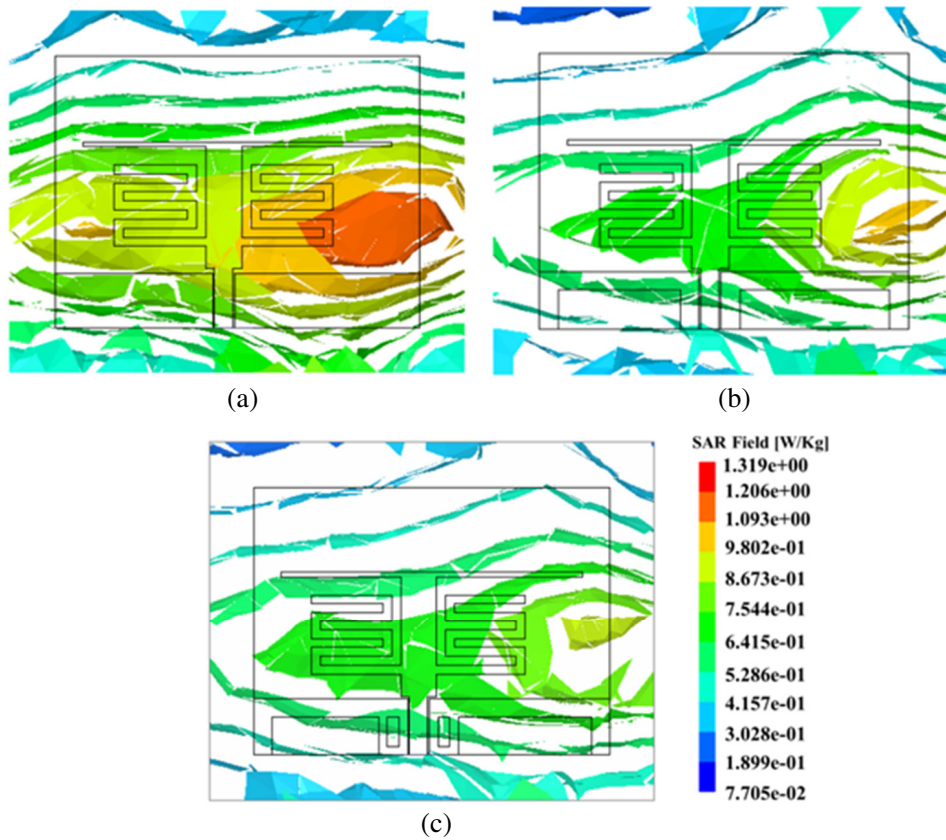

Figure 8. SAR plots with hand model in HFSS, (a) simple ground, (b) inverted U-shape ground, (c) truncated ground.

Figure 7(d) shows the direction of heat flux generated due to the application of the antenna. The symmetrical meander line antenna is simulated with hand phantom model in ANSYS HFSS software where the dielectric parameters at the given operating frequency are obtained from [16].

The results of the simulation, when the antenna is placed at a distance of 15 mm, form the hand phantom model and are shown in Fig. 8. It is observed that the SAR decreases with hand phantom modeled in HFSS from 1.31 Watt/Kg to 0.98 Watt/Kg with the application of truncated ground plane in the proposed antenna. The values of SAR obtained in two solvers are not the same due to the different geometries of the body in two cases. When a human body is exposed to electromagnetic waves, due to the lossy nature of the tissue, a part of the energy gets absorbed within the body and results in temperature elevation. So temperature profile has also been taken into consideration while designing wearable antennas.

7. TEMPERATURE ANALYSIS

Heating effect due to electromagnetic waves absorption is harmful and can damage the cells, but if it is lower than the threshold limit of 1 K, then it is normal. The heat transfer equation in tissues without thermoregulation is given by [17] which is:

$$\rho c \frac{\partial T'}{\partial t} = k \nabla^2 T' - V_s(T' - T_0) + Q \tag{4}$$

The differential temperature rise $(T' - T_0)$ is represented with T. The overall equation can be rewritten as:

$$\mu \frac{\partial T}{\partial t} = \nabla^2 T - \lambda_s T + Q \tag{5}$$

where

$$\mu = \frac{\rho c}{k}, \quad \lambda_s = \frac{V}{k}, \quad Q = \frac{\rho \text{SAR}}{k}, \quad V = \rho_b c_b \rho \omega$$

ρ = Specific density of brain tissue in kg/m^3, k = Thermal conductivity of the tissue in Watt/m/°C, c = Heat capacity of the tissue in J/Kg/°C, V_S = Product of flow and heat capacity of blood in Watt/m^3/°C, Q = Heat input due to electromagnetic wave in Watt/m^3, T' = Enhanced temperature in °C, T_o = Ambient blood temperature in °C, ρ_b = Specific density of blood in kg/m^3, c_b = Heat capacity of the blood in J/Kg/°C, ω = Blood perfusion rate in brain tissues, SAR = Specific absorption rate.

In [17], a spherical active region of radius $\lambda/4$ is taken to study the phenomenon of heat transfer in head tissues. In our case for studying the effects of radiation over head of a child, the operating frequency of the antenna is taken as 2.5 GHz. The result of the analysis is given in Fig. 9. It can be observed that maximum temperature increase inside the head is merely 0.42 K which is less than the threshold of 1 K.

Thus the above analysis about SAR and temperature dependency with various parameters gives an insight about the effect of electromagnetic waves from the antenna inside human body which is an
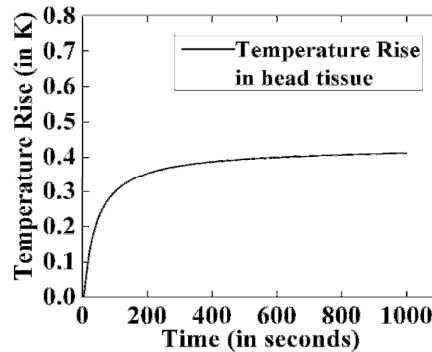

Figure 9. Temperature elevation plot with time.

Table 2. Comparative studies.

Reference	Reduction Technique	Impedance Bandwidth	Separation Distance (From Body)	Volume	Antenna Complexity	Reduction
[18], 2009	Metamaterial	-	25 mm		Bulky Structure	57.89%
[19], 2011	Electromagnetic Band gap	-	10 mm	$35 \times 51 \times 4.5$	Bulky Structure	84%
[20], 2014	Current Slope Discontinuity Reduction	5.5%	-	$90 \times 50 \times 0.6$	Simple	10%
[21], 2015	Larger Gnd. Plane & High ε_r Substrate	35%	-	$157.5 \times 88 \times 9.1$	Simple	35%
[22], 2015	Metamaterial cover	5% and 3.6%	15 mm	$24.8 \times 24.8 \times 5.4$	Bulky Structure	93%
Proposed	E-Field Cancellation	69.04%	15 mm	$30 \times 40 \times 1.6$	Simple	25.5% (HFSS)

important factor while designing wearable antennas. Finally, the designed antenna is comprehensively compared with other antennas designed in the past. The comparative study is shown in Table 2. Compared to the earlier designed antennas, the proposed SAR reduction technique is efficient in terms of compactness as no additional unit is required for the purpose. Bandwidth enhancement is also found to be a noted achievement with this design.

8. CONCLUSION

In this paper, bandwidth enhancement and SAR reduction technique of CPW-fed symmetrical meander line wearable antenna with truncated ground planes is discussed. Excitation of higher order mode and miniaturization of this mode with the lower mode results in enhanced bandwidth. Further SAR value which is the most important factor for wearable antennas is reduced significantly through the application of truncated ground planes. The temperature profile of the antenna is also evaluated and found to be within the threshold temperature limit. The radiation pattern of the antenna is found to be good with radiation efficiency of 96.9%. The proposed antenna is found to be viable for real world applications.

ACKNOWLEDGMENT

REFERENCES

1. Behdad, N. and K. Sarabandi, "Bandwidth enhancement and further size reduction of a class of miniaturized slot antennas," *IEEE Trans. on Antennas and Propag.*, Vol. 52, No. 8, 1928–1935, Aug. 2004.

2. Mitra, D., D. Das, and S. R. Bhadra Chaudhuri, "Bandwidth enhancement of microstrip line and CPW-fed asymmetrical slot antennas," *Progress In Electromagnetics Research Letters*, Vol. 32, 69–79, 2012.

3. Furuya, K., Y. Taira, and H. Iwasaki, "Wide band wearable antenna for DTV reception," *IEEE Int. Symp. AP-S*, San Diego, U.S.A, Jul. 2008.

4. Isogai, E., Y. Okano, S. Yamamoto, N. Tamaki, T. Harada, A. Kuramoto, and T. Taura, "Research of wideband wearable antenna integrated on the clothing," *ISAP 2008 Proceedings*, Taiwan, 2008.

5. Wang, J. and O. Fujiwara, "Reduction of electromagnetic absorption in the human head for portable telephones by a ferrite sheet attachment," *IEICE Trans. Commun.*, Vol. E80B, No. 12, 1810–1815, Dec. 1997.

6. Hwang, J. N. and F. C. Chen, "Reduction of the peak SAR in the human head with metamaterials," *IEEE Trans. on Antennas and Propag.*, Vol. 54, No. 12, 3763–3770, Dec. 2006.

7. Zhu, S. and R. Langley, "Dual-band wearable textile antenna on an EBG substrate," *IEEE Trans. on Antennas and Propag.*, Vol. 57, No. 4, 926–935, Apr. 2009.

8. Haridim, M., "Use of rod reflectors for SAR reduction in human head," *IEEE Trans. on Electromagnetic Compatibility*, Vol. 58, No. 1, 40–46, Nov. 2015.

9. Mageed, M. A., C. Pelleti, and R. Mittra, "Penta-band PIFA for SAR reduction for mobile and WLAN applications using R-card," *IEEE International Symposium on Antennas and Propag. & USNC/URSI National Radio Science Meeting*, Vancouver, BC, 2015.

10. Han, K., M. Swaminathan, R. Pulugurtha, H. Sharma, R. Tummala, S. Yang, and V. Nair, "Magneto-dielectric nano composite for Antenna Miniaturization and SAR reduction," *IEEE Antennas and Wireless Propag. Letters*, Vol. 15, 72–75, May 2015.

11. Garg, R., P. Bhartia, I. Bahl, and A. Ittpiboon, *Microstrip Antenna Design Handbook*, Artech House Incl., 2001.

12. Tsai, C. L., K. W. Chen, and C. L. Yang, "Implantable wideband low-SAR antenna with C-shaped coupled ground," *IEEE Antennas and Wireless Propag. Letters*, Vol. 14, 1594–1597, Aug. 2015.

13. *IEEE Standard for Safety Levels With Respect to Human Exposure to Radio Frequency Electromagnetic Fields, 3 kHz to 300 GHz*, IEEE Standard C95.1-2005, 2006.

14. Yang, T., W. A. Davis, W. L. Stutzman, and M. C. Huynh, "Cellular-phone and hearing-aid interaction, an antenna solution," *IEEE Antennas and Propag. Mag.*, Vol. 50, No. 3, 51–65, Jun. 2008.

15. Calla, O. P. N., A. Singh, A. K. Singh, S. Kumar, and T. Kumar, "Empirical relation for designing the meander line antenna," *Proceedings of International conference on Microwave*, Jaipur, India, 2008.

16. Andreuccetti, D., R. Fossi, and C. Petrucci, "An internet resource for the calculation of the dielectric properties of body tissues in the frequency range 10 Hz–100 GHz," Website at http://niremf.ifac.cnr.it/tissprop/.IFAC-CNR, Florence, Italy, 1997, based on data published by C. Gabriel, et al. in 1996.

17. Kritikos, H. N. and H. P. Schwan, "Potential temperature rise induced by electromagnetic field in brain tissues," *IEEE Trans. on Biomedical Engg.*, Vol. 26, No. 1, 29–34, Jan. 1979.

18. Manapati, M. B. and R. S. Kshetrimayum, "SAR reduction in human head from mobile phone radiation using single negative metamaterials," *Journal of Electromagnetic Waves and Applications*, Vol. 23, 1385–1395, 2009.

19. Ikeuchi, R. and A. Hirata, "Dipole antenna above EBG substrate for local SAR reduction," *IEEE Antennas and Wireless Propag. Letters*, Vol. 10, 904–906, 2011.

20. Choi, W. C., K. J. Kim, Y. J. Yoon, and J. U. Ha, "Inverted-F antenna with modified current distribution for SAR reduction," *Antenna Technology International Workshop*, 36–39, Sydney, NSW, Australia, 2014.

21. Trajkovikj, J. and A. Skrivervik, "Diminishing SAR for wearable UHF antennas," *IEEE Antennas and Wireless Propag. Letters*, Vol. 14, 1530–1533, 2015.

22. Rosaline, S. I. and S. Raghavan, "A compact dual band antenna with an ENG SRR cover for SAR reduction," *Microwave Optical Technology Letter*, Vol. 57, 741–747, 2015.